Inorganic Chemistry

Article

pubs.acs.org/IC

Photocatalytic CO_2 Reduction to Formic Acid Using a Ru(II)−Re(I) Supramolecular Complex in an Aqueous Solution

Akinobu Nakada,[†] Kazuhide Koike,[‡,§] Takuya Nakashima,[†] Tatsuki Morimoto,[†,§,∇] and Osamu Ishitani*[,†,§]

[†]Department of Chemistry, Graduate School of Science and Engineering, Tokyo Institute of Technology, 2-12-1-NE-1 O-okayama, Meguro-ku, Tokyo 152-8550, Japan

[‡]National Institute of Advanced Industrial Science and Technology, 16-1 Onogawa, Tsukuba 305-8569, Japan

[§]CREST, Japan Science and Technology Agency (JST), 4-1-8 Honcho, Kawaguchi, Saitama 332-0012, Japan

Supporting Information

ABSTRACT: In an aqueous solution, photophysical, photochemical, and photocatalytic abilities of a Ru(II)−Re(I) binuclear complex (**RuReCl**), of which Ru(II) photosensitizer and Re(I) catalyst units were connected with a bridging ligand, have been investigated in details. **RuReCl** could photocatalyze CO_2 reduction using ascorbate as an electron donor, even in an aqueous solution. The main product of the photocatalytic reaction was formic acid in the aqueous solution; this is very different in product distribution from that in a dimethylformamide (DMF) and triethanolamine (TEOA) mixed solution in which the main product was CO. A $^{13}CO_2$ labeling experiment clearly showed that formic acid was produced from CO_2. The turnover number and selectivity of the formic acid production were 25 and 83%, respectively. The quantum yield of the formic acid formation was 0.2%, which was much lower, compared to that in the DMF−TEOA mixed solution. Detail studies of the photochemical electron-transfer process showed back-electron transfer from the one-electron-reduced species (OERS) of the photosensitizer unit to an oxidized ascorbate efficiently proceeded, and this should be one of the main reasons why the photocatalytic efficiency was lower in the aqueous solution. In the aqueous solution, ligand substitution of the Ru(II) photosensitizer unit proceeded during the photocatalytic reaction, which was a main deactivation process of the photocatalytic reaction. The product of the ligand substitution was a Ru(II) bisdiimine complex or complexes with ascorbate as a ligand or ligands.

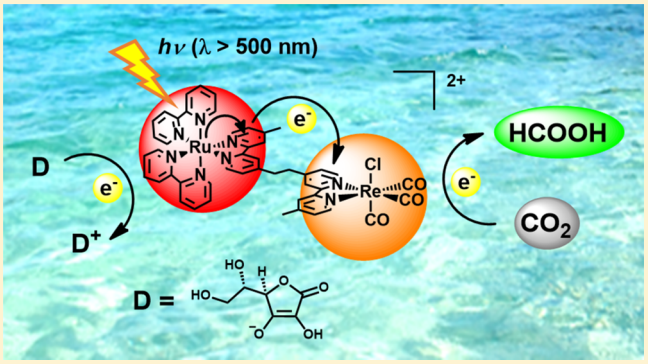

INTRODUCTION

Human beings are facing three serious problems, i.e., global warming and shortages of the carbon and energy resources. To solve these problems, the conversion of solar energy to chemical energy using CO_2 reduction photocatalysts has been tremendously interesting. For practical use, water should be an electron source for CO_2 reduction, because it is a very abundant resource. In other words, the photocatalysts should work in an aqueous solution. However, there have been only a few reports for photocatalytic systems that can work for CO_2 reduction in an aqueous solution, even though a sacrificial reductant is used. Photocatalytic systems of Ni(II)[1−6] and Co(II)[6] macrocyclic complexes as CO_2 reduction catalysts with a $[Ru(N^N)_3]^{2+}$ photosensitizer (N^N = diimine ligand) and ascorbate as a reductant can reduce CO_2 in an aqueous solution; however, the durability of the photocatalytic systems was very low (turnover number (TON) of 0.01−4.8) and a considerable amount of H_2 was also produced. MacDonnell and co-workers recently reported that pyridine drove photocatalytic CO_2 reduction with the similar photosensitizer and sacrificial electron donor (ascorbate) in an aqueous solution.[7] Murata and co-workers investigated a vesicle system containing a Ru(II) photosensitizer and a Re(I) catalyst for CO_2 reduction.[8] This system also used ascorbate as a reductant and produced CO selectively.

We have reported supramolecular photocatalysts with both a Re(I) complex as a catalytic unit and a $[Ru(N^N)_3]^{2+}$ complex as a photosensitizer unit (see Chart 1 as an example), which can reduce CO_2 selectivity to CO in a dimethylformamide and triethanolamine (DMF−TEOA) mixed solution under visible-light irradiation.[9−13] They are efficient photocatalysts with high durability (the quantum yield and the turnover number of CO formation were up to 21% and over 232, respectively, in the case using 1-benzyl-1,4-dihydronicotinamide (BNAH) as a sacrificial electron donor, respectively).[10] On the other hand, a similar supramolecular photocatalyst constructed with two different Ru(II) complex units, which works as a photosensitizer or a catalyst, selectively producing formic acid as a

Received: November 10, 2014
Published: February 5, 2015

DOI: 10.1021/ic502707t
Inorg. Chem. 2015, 54, 1800−1807

Chart 1. Structures and Abbreviation of the Ru(II)−Re(I) Supramolecular Photocatalyst RuReCl and the Corresponding Model Complexes Ru and ReCl

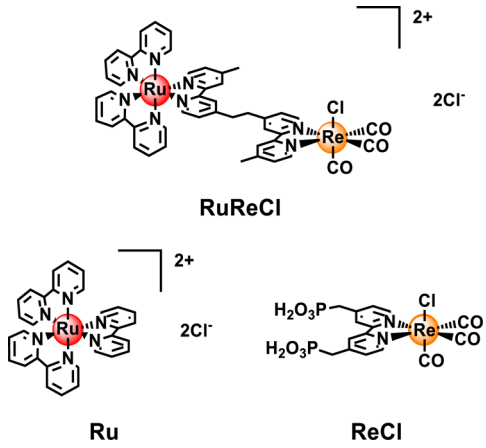

main reduction product of CO_2.[14] This was hybridized with a semiconductor photocatalyst, Ag-loaded TaON, which exhibits a strong photo-oxidation power. This hybrid system photocatalyzes CO_2 reduction in methanol, which works as both a solvent and a sacrificial reductant, via the Z-scheme mechanism; that is, excitation of both the Ru(II) photosensitizer and TaON induces CO_2 reduction.[15] One of the next processes investigated for such Z-scheme photocatalysts should be the achievement of photocatalytic CO_2 reduction with water as a reductant. However, photochemical properties and photocatalytic abilities of the supramolecules have not been known in an aqueous solution. We herein report the photocatalysis of **RuReCl** (Chart 1) for CO_2 reduction in an aqueous solution. This system actually worked as a photocatalyst for CO_2 reduction using ascorbate as a reductant in aqueous solution as well, but the main product was HCOOH, rather than CO.

RESULTS AND DISCUSSION

To start the investigation of the photocatalysis in an aqueous solution, sacrificial electron donors should be examined, because BNAH[9−13] and a benzoimidazole derivative (BIH[16]), which have been widely used as reductants in organic solutions, do not solve in water. Ascorbic acid, sodium ascorbate, TEOA, NaI, $FeCl_2$, and glucose were examined as quencher of the excited **Ru** unit of **RuReCl**, and only sodium ascorbate could efficiently quench the emission from the **Ru** unit, but the others did not. The different quenching rate constants of the excited **Ru** by ascorbate have been reported in some papers.[17−19] We determined the quenching rate constant by the Stern−Volmer plots using emission strengths, which showed a good linearity shown in Figure S1 in the Supporting Information, as described later. It should be noted that, even using sodium ascorbate (200 mM in the photocatalytic reaction condition), the pH of the solution was 5.5 after CO_2 bubbling, in which the concentrations of ascorbate and ascorbic acid were calculated to be 190 mM and 10 mM, respectively, using the pK_{a1} value of ascorbic acid (4.17).[20]

As a typical run, an aqueous solution containing **RuReCl** (0.05 mM) and sodium ascorbate (200 mM) was irradiated at λ > 500 nm under a CO_2 atmosphere, where pH of the solution was 5.5 after the CO_2 bubbling. Formic acid was produced with 83% selectivity and small amounts of CO and H_2 were detected (Figure 1). The turnover number (TON) of formic acid

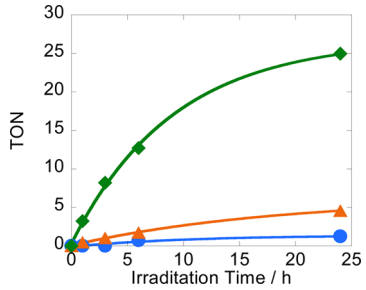

Figure 1. Turnover number (TON) values of HCOOH (green), CO (blue), and H_2 (orange) in the photocatalytic reaction using **RuReCl**. An aqueous solution containing **RuReCl** (0.05 mM) and sodium ascorbate (200 mM) was irradiated at λ > 500 nm under a CO_2 atmosphere.

reached 25 (1.2 for CO, 4.6 for H_2) after 24-h irradiation. The quantum yield was 0.2% using 546 nm monochromatic light (Figure S2). On the other hand, only a small amount of formic acid was produced (TON_{HCOOH} = 1.9) when a 1:1 mixed system of the corresponding mononuclear model complexes (**Ru** and **ReCl** in Chart 1) was used. This shows that the connection of the photosensitizer with the catalyst should be important for the photocatalytic reduction of CO_2 in an aqueous solution as well. It is also noteworthy that the product distribution in the aqueous solution (mainly formic acid) was very different from that in the DMF−TEOA mixed solution (selectively CO; see Figure S3 in the Supporting Information).

To identify the carbon source of formic acid, a $^{13}CO_2$ labeling experiment was conducted. Under a $^{13}CO_2$ atmosphere (707 Torr), an aqueous solution containing **RuReCl** (0.5 mM) and sodium ascorbate (200 mM) was irradiated under the same conditions as those described above. Figure 2 shows ^{13}C NMR

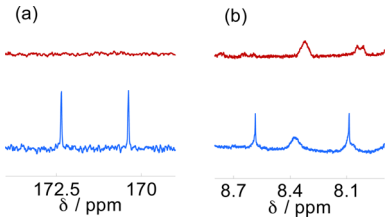

Figure 2. (a) No-D ^{13}C NMR and (b) ^{1}H NMR spectra of the reaction solution before (red) and after (blue) 18 h of irradiation. An aqueous solution containing **RuReCl** (0.5 mM) and sodium ascorbate (200 mM) was irradiated at λ > 500 nm under a $^{13}CO_2$ atmosphere (707 Torr).

and ^{1}H NMR spectra measured by a standard solvent method (No-D) before and after irradiation for 18 h. After the irradiation, a doublet ($^{1}J_{CH}$ = 195 Hz) at 171.5 ppm, which was attributed to the ^{13}C in $H^{13}COOH$, was observed in the ^{13}C NMR spectrum while no peak was detected at this area before irradiation. The methine proton of $H^{13}COOH$ was also observed as a doublet ($^{1}J_{CH}$ = 195 Hz) at 8.35 ppm in the ^{1}H NMR spectrum after irradiation. These clearly show that formic acid was photocatalytically produced by reduction of CO_2.

Table 1 summarizes the photophysical properties of the complexes in aqueous solutions. Absorption and emission spectra of **RuReCl** and **Ru**, and an absorption spectrum of **ReCl** are shown in Figure 3. The absorption bands with λ_{max} = 340 and 456 nm are attributable to the ^{1}MLCT transition of

DOI: 10.1021/ic502707t
Inorg. Chem. 2015, 54, 1800−1807

Table 1. Photophysical Properties of the Metal Complexes in Water at 298 K and Their Quenching Behaviors by Sodium Ascorbate

	λ_{abs}/nm (ε_{max}/× 10^3 M^{-1} cm^{-1})						
complex	$\pi-\pi^*$	MLCT	$\lambda_{em}{}^a$ (nm)	$\tau_{em}{}^a$ (ns)	$\Phi_{em}{}^a$	$k_q{}^b$ (× 10^7 M^{-1} s^{-1})	$\eta_q{}^{b,c}$
RuReCl	287 (83.3)	456 (13.4)	628	561	0.055	13.7	0.94
Ru	286 (74.6)	452 (12.7)	625	580	0.060	6.28	0.87
ReCl	319 (14.0), 307 (13.4)	340 (4.9)	*d*				

[a]Measured under an argon atmosphere, using 456-nm excitation light. [b]See ref 20. [c]Quenching efficiency of emission under the photocatalytic reaction condition. [d]Emission was not observed because **ReCl** could not absorb the 456-nm light.

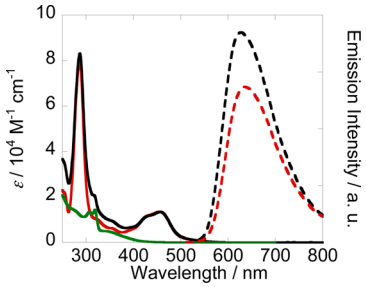

Figure 3. Absorption (solid line) and emission spectra (broken line) of **RuReCl** (black), **Ru** (red), and **ReCl** (green) in water.

the **Ru** and Re units, respectively, and the $^1\pi-\pi^*$ absorption bands of each units were observed at λ_{max} = 287 nm and ~310 nm. The absorption spectrum of **RuReCl** was very similar to the summation spectrum of the corresponding model complexes. In the emission spectrum from the ^{3}MLCT excited state of **RuReCl**, on the other hand, the maximum was red-shifted by 3 nm, the quantum yield was lower, and the lifetime was shorter, compared with those of **Ru**. The similar phenomena were observed in an organic solution, and they are caused by weak electronic interaction between the **Ru** and Re unit in cases of some Ru(II)−Re(I) supramolecules, which were connected by the same bridging ligand.[11,12]

The ^{3}MLCT excited state of **RuReCl** was quenched by sodium ascorbate. The quenching parameters of emission from **RuReCl** and **Ru**, which were obtained using the linear Stern−Volmer plots (seeFigure S1 in the Supporting Information) and the luminescence lifetimes (τ_{em}), are also summarized in Table 1. The quenching rate constant (k_q) and quenching efficiency (η_q) in the photocatalytic reaction condition for **RuReCl** were larger and higher, respectively, compared to those of **Ru**, because the oxidative power of **RuReCl** is stronger in the excited state than **Ru**, because of the intramolecular electronic interaction.[11,12]

We attempted to measure the absorption attributable to the reduced species of **RuReCl** such as $[Ru^{II}(N^{\wedge}N)_2(N^{\wedge}N^-)]^+$ and/or $[Re^{I}(N^{\wedge}N^-)(CO)_3Cl]^-$ that are produced by photo-induced electron transfer from a sacrificial reductant during the photocatalytic reaction. However, in the UV-vis absorption spectra during photocatalytic reaction, no absorption change was observed at the first stage of the reaction in an aqueous solution containing sodium ascorbate (200 mM), as shown in Figure 4a. Conversely, in a DMF-TEOA (5:1 v/v) mixed solution containing BNAH (100 mM) as a reductant, the absorption at wavelengths longer than 470 nm, attributable to the one-electron-reduced species (OERS) of **RuReCl**, where the added electron should be localized primarily on the **Ru** unit, because of the similarity of the UV-vis absorption spectrum to the OERS spectrum of **Ru** (see Figure 4d),[9] could be clearly observed, even immediately after irradiation commenced (see

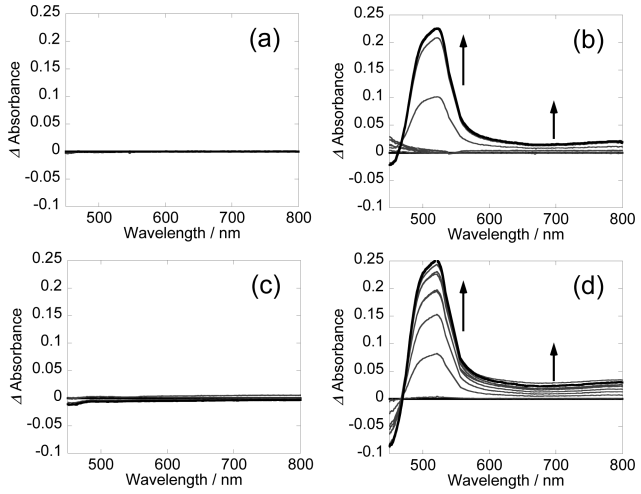

Figure 4. UV-vis absorption spectral changes of solutions containing a complex and a reductant during irradiation at λ = 546 nm (2.8×10^{-7} einstein/s) under a CO_2 atmosphere: (a) an aqueous solution containing **RuReCl** (0.05 mM) and sodium ascorbate (200 mM), irradiation time 0−5 min (60 s intervals); (b) a DMF−TEOA (5:1) solution containing **RuReCl** (0.05 mM) and BNAH (100 mM), irradiation time 0−1.5 min (10 s intervals); (c) an aqueous solution containing **Ru** (0.05 mM) and sodium ascorbate (200 mM), irradiation time 0−5 min (60 s intervals); (d) a DMF−TEOA (5:1) solution containing **Ru** (0.05 mM) and BNAH (100 mM), irradiation time 0−1.5 min (10 s intervals).

Figure 4b). There are two possible reasons for this difference. One is very efficient back-electron transfer (BET) from the OERS of the **Ru** unit to the oxidized ascorbate in the aqueous solution. Another is more rapid consumption of the added electron for CO_2 reduction in the aqueous solution than that in the organic solution. To clarify these reasons, similar experiments were done on **Ru**, which should not use electron for CO_2 reduction. Figures 4c and 4d show the absorption changes of **Ru** in an aqueous solution containing sodium ascorbate (η_q = 0.87) and in a DMF−TEOA (5:1 v/v) mixed solution containing BNAH (η_q = 0.97), respectively. No spectral change was observed in the aqueous solution though the OERS was clearly accumulated in the organic solution, therefore, the BET from the OERS of **Ru** to the oxidized ascorbate should be more efficient in water.

To clarify the details of the photochemical redox processes, laser-flash-photolysis experiments of **Ru** were conducted. Transient absorption spectra of **Ru** measured after laser excitation are shown in Figure 5. In the case of an aqueous solution in the absent of any electron donor, new absorption band with λ_{max} = 368 nm appeared with bleaching of the broad absorption at ~460 nm, attributable to a decrease in the ground state of **Ru** (see Figure 5a). This can be identified as formation

DOI: 10.1021/ic502707t
Inorg. Chem. 2015, 54, 1800−1807

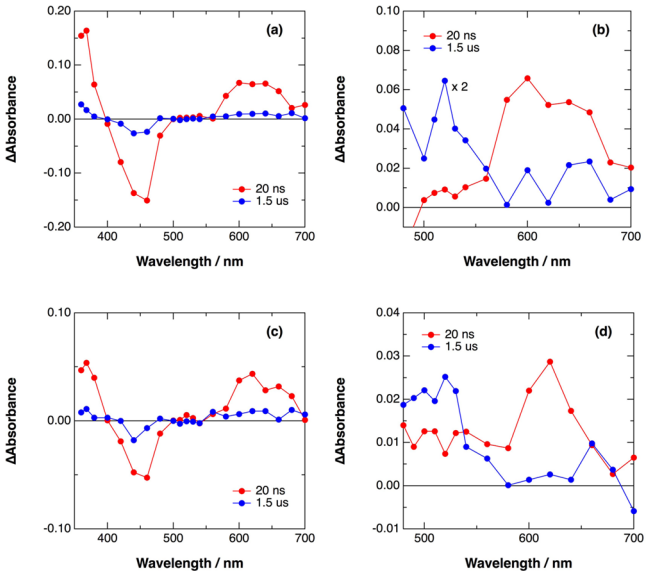

Figure 5. Transient UV-vis absorption spectra 20 ns (red) and 1.5 μs (blue) after laser excitation: aqueous solutions containing **Ru** (0.05 mM) (a) without and (b) with sodium ascorbate (200 mM) were irradiated at λ = 430 nm; DMF−TEOA (5:1 v/v) mixed solutions containing **Ru** (0.05 mM) (c) without and (d) with BNAH (100 mM) were irradiated at λ = 480 nm. The solutions were degassed by bubbling with argon, and then they were irradiated at room temperature.

of the ^{3}MLCT excited state of **Ru** (**Ru***), by comparison with the previous report.[21] In the presence of sodium ascorbate (200 mM), the bands of the **Ru*** (red line in Figure 5b) rapidly disappeared and a new absorption band with λ_{max} = 510 nm appeared, which is attributable to the OERS of **Ru** (**Ru**$^-$) (blue line in Figure 5b).[21] These results clearly show that **Ru*** formed by irradiation was reductively quenched by ascorbate to produce the OERS. Although similar transient absorption spectra were observed in DMF−TEOA (5:1 v/v) with or without BNAH (100 mM), respectively see Figures 5c and 5d), the formation yield of **Ru**$^-$ was very different from that in the aqueous solution, as described later.

Figure 6 illustrates time conversion curves of **Ru**$^-$ after the 532-nm laser flash in the presence of the electron donors, where the absorbance on the vertical axis is normalized by both the laser power and the absorbance of the ground state of **Ru** at

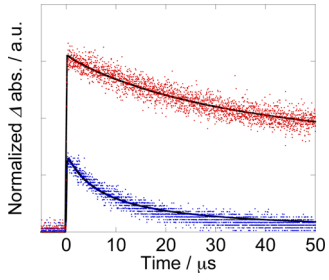

Figure 6. Time profiles of **Ru**$^-$: an aqueous solution containing **Ru** (0.2 mM) and sodium ascorbate (200 mM, blue), and a DMF-TEOA (5:1 v/v) mixed solution containing **Ru** (0.2 mM) and BNAH (100 mM, red) were irradiated using 532 nm laser light under degassed conditions at room temperature. The absorbance on the vertical axis is normalized by both the laser power and the absorbance of the ground state of **Ru** at 532 nm.

532 nm. This result clearly shows that the formation yield of **Ru**$^-$ just after the laser flash in the aqueous solution using sodium ascorbate was much lower than that in the DMF−TEOA solution using BNAH. Based on the molar absorption coefficients of **Ru*** at 368 nm and **Ru**$^-$ at 510 nm (2.5×10^4 M^{-1} cm^{-1} and 1.2×10^4 M^{-1} cm^{-1}, respectively),[21] the formation yields of **Ru**$^-$ just after escaping from the solvent cage (Φ_{OERS}^{escape}) were calculated as 0.37 in the aqueous solution and 0.82 in the DMF−TEOA solution using eq 1. Since the quenching efficiencies (η_q) were similar in both solutions (η_q = 0.87 by sodium ascorbate in the aqueous solution and 0.97 by BNAH in the DMF−TEOA solution), this result clearly shows that the cage escape efficiency (η_{cage}, eq 1) in the aqueous solution was a factor of 2 lower than that in the DMF−TEOA solution (see Table 2). This cage escape yield (0.42) is similar to the value reported by Krishnan and Sutin (0.5).[22]

$$\Phi_{OERS}^{escape} = \frac{[\mathbf{Ru}^-]_0}{[\mathbf{Ru}^*]_0} = \eta_q \times \eta_{cage} \quad (1)$$

Table 2. Photoinduced Electron Transfer Reactions between Ru and a Reductant

solvent	reductant	Φ_{OERS}^{escape}	η_q	η_{cage}	k_{bet2} ($\times 10^9$ M^{-1} s^{-1})
water	sodium ascorbate (200 mM)	0.37	0.87	0.43	15.1
DMF−TEOA	BNAH (100 mM)	0.82	0.97	0.85	1.15

The time courses of **Ru**$^-$ could be fitted (see the Supporting Information) using the kinetics shown in Scheme 1; the

Scheme 1. Reaction Pathways of the Photochemical Reaction of Ru with Sodium Ascorbate in an Aqueous Solution (Blue) and with BNAH in a DMF−TEOA Mixed Solution (Green)

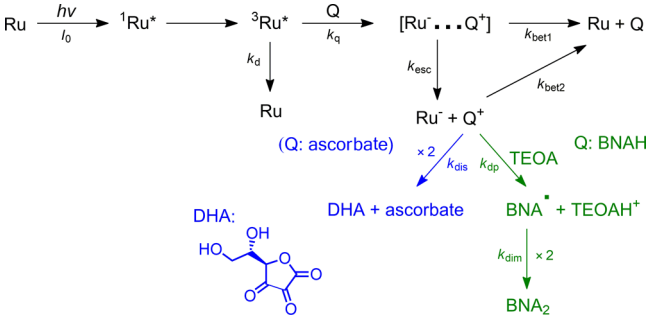

pseudo-first-order rate constant of increase in **Ru**$^-$ in the aqueous solution was 9.0×10^6 s^{-1}, which corresponds to the product of the quenching rate by sodium ascorbate and the cage escape yield (k_q[Q: 0.2 M]η_{cage} = 5.5×10^6 s^{-1}). This also strongly supports that **Ru**$^-$ was produced by the photoinduced electron transfer from ascorbate to **Ru***.

After escaping from the solvent cage, both BET from **Ru**$^-$ to the ascorbate radical (Asc$^\bullet$) in the aqueous solution and BNAH$^{+\bullet}$ in the DMF−TEOA appeared to act as diffusion control processes (k_{bet2}(Asc$^\bullet$) = 15.1×10^9 M^{-1} s^{-1}; k_{bet2}(BNAH$^{+\bullet}$) = 1.15×10^9 M^{-1} s^{-1}). The higher viscosity of the DMF (0.794 mPa s)[23]−TEOA (609 mPa s)[23] mixed solution, because of the considerably higher viscosity of the TEOA, could have caused these processes to occur at a rate

DOI: 10.1021/ic502707t
Inorg. Chem. 2015, 54, 1800−1807

slower than that in water (0.890 mPa s).[23] Moreover, the speeds of the decomposition reactions for $BNAH^{+\bullet}$ and $Asc^{\bullet}$ should considerably affect the survival yield of $\mathbf{Ru}^{-}$ in solution. Proton capture from $BNAH^{+\bullet}$ by TEOA produced $BNA^{\bullet}$ with $k_{dp} = 3.01 \times 10^{3}\ M^{-1}\ s^{-1}$ in the DMF−TEOA (5:1 v/v), and it has been reported that quantitative dimerization of $BNA^{\bullet}$ produces stable compounds, e.g., BNA_2.[16] Although the deprotonation process is slow, under photocatalytic reaction conditions, the deprotonation from $BNAH^{+\bullet}$ sufficiently competes with the BET from $\mathbf{Ru}^{-}$ to $BNAH^{+\bullet}$, because the deprotonation is a pseudo-first-order process affecting $[BNAH^{+\bullet}]$ ([TEOA] = 1.3 M). Furthermore, concentrations of both $\mathbf{Ru}^{-}$ and $BNAH^{+\bullet}$ should be very low during irradiation. On the other hand, the main decomposition process of $Asc^{\bullet}$ has been reported to be the disproportionation of $Asc^{\bullet}$, which produces dehydroascorbic acid (DHA) and ascorbate. Because the disproportionation process is considerably slower ($k_{dis} = 8 \times 10^{7}\ M^{-1}\ s^{-1}$) than the BET,[24] this should also lower the survival yield of free $\mathbf{Ru}^{-}$ in the aqueous solution, compared with that in the DMF−TEOA solution. It is noteworthy that DHA potentially works as an oxidant of $\mathbf{Ru}^{-}$,[25−27] and this process may have lowered the accumulated yield of $\mathbf{Ru}^{-}$ during irradiation.

In summary of this section, the aqueous system using ascorbate has the following disadvantages for producing and accumulating $\mathbf{Ru}^{-}$, compared to the DMF−TEOA system using BNAH: (1) lower escape yield of $\mathbf{Ru}^{-}$ from the solvent cage, (2) faster BET (depending on the diffusion rate) from $\mathbf{Ru}^{-}$ to $Asc^{\bullet}$, and (3) slower decomposition process of the $Asc^{\bullet}$. They should also lower the efficiency of the photocatalytic CO_2 reduction.

The production yield of the free OERS of the **Ru** unit of **RuReCl** in the aqueous solution was also much lower, compared with that in the DMF−TEOA solution as described above, probably because of the similar rapid BET processes. This should be one of the main reasons why the quantum yield of CO_2 reduction using **RuReCl** in the aqueous solution containing sodium ascorbate (Φ_{HCOOH} = 0.2%) was much lower than that in the DMF−TEOA mixed solution containing BNAH (Φ_{CO} = 12.6%). The saturated concentration of CO_2 dissolved in water (34 mM at 298 K) is ∼6 times lower than that in the DMF solution.[28] This could be another reason why the photocatalysis of **RuReCl** was lower in the aqueous solution; however, currently, there is no experimental evidence in this regard.

Figure 7 shows the dependence of the photocatalytic formation of formic acid on the photon flux of 546-nm monochromatic light. The higher photon flux caused the more-efficient formation of formic acid. This suggests that the faster production of the OERS of the photocatalyst induced the higher Φ_{HCOOH} value. In other words, the formation of the reduced species of the photocatalyst might be a rate-limiting process in the aqueous solution. Given this consideration, an addition effect of **Ru** into the photocatalytic reaction solution was investigated as follows. In the presence or absence of **Ru** (0.05−0.5 mM), the reaction solutions containing **RuReCl** (0.05 mM) and sodium ascorbate (200 mM) were irradiated at λ > 500 nm for 24 h. Table 3 shows amounts of formic acid produced in these reactions. Under this reaction condition, the light of a mercury lamp (546 nm) was mainly absorbed by both **Ru** and **RuReCl**. Note that the absorbance of **RuReCl** at λ = 546 nm was 0.032, but that of the reaction solutions was up to 0.25, because of the presence of **Ru** (see Table 3); therefore,

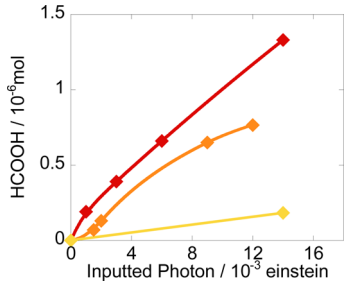

Figure 7. Light-intensity dependence of formation of formic acid in the photocatalytic reaction using **RuReCl** (0.05 mM) and sodium ascorbate (200 mM): aqueous solutions were irradiated at λ = 546 nm under CO_2 atmosphere. The light intensities were 2.8×10^{-7} einstein s^{-1} (red), 1.4×10^{-7} einstein s^{-1} (orange), and 0.56×10^{-7} einstein s^{-1} (yellow), respectively.

Table 3. Photocatalytic Formation of Formic Acid in the Absence and in the Presence of Ru[a]

run	[Ru] (mM)	HCOOH (μmol)	$A_{546\ nm}$[b]
1	0	4.4	0.032
2	0.05	6.0	0.054
3	0.1	7.4	0.076
4	0.5	11	0.25
5[c]	0.5	0.11	0.22

[a]Aqueous solutions containing **RuReCl** (0.05 mM), various concentrations of **Ru**, and sodium ascorbate (200 mM) were irradiated at λ > 500 nm for 24 h under a CO_2 atmosphere. [b]Absorbance of the reaction solution at 546 nm. [c]In the absence of **RuReCl**.

the addition of **Ru** should suppress the photocatalytic formation of formic acid, because of its internal filtering effect if **Ru** would not have a positive role or roles in the photocatalytic reaction. However, the addition of **Ru** clearly accelerated the photocatalytic formation of formic acid, which was enhanced in the presence of the higher concentration of **Ru**. This is probably because the addition of **Ru** opened up a new electron supply route to the photocatalyst.

The turnover number of the **RuReCl** photocatalyst was much lower in the aqueous solution (TON_{HCOOH} = 25 for 24-h irradiation; see Figure 1), compared with that in the DMF−TEOA mixed solution (TON_{CO} = 110 for 24-h irradiation; see Figure S3 in the Supporting Information). Figure 8 shows differential UV−vis absorption spectra of the photocatalytic reaction solution using **RuReCl** between before and after irradiation. After the irradiation, the ^{1}MLCT absorption band of the photosensitizer unit (λ_{max} = 456 nm) was decreased and a new absorption band at λ_{max} = 525 nm appeared. This spectral

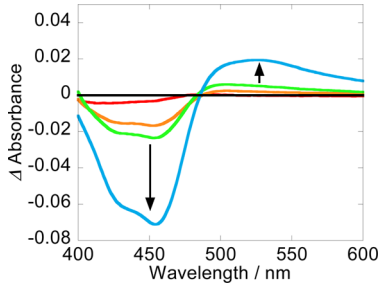

Figure 8. Differential absorption spectra of the photocatalytic reaction solution using **RuReCl** between before and after irradiation (1, 3, 6, and 24 h). The reaction condition was described in Figure 1.

DOI: 10.1021/ic502707t
Inorg. Chem. 2015, 54, 1800−1807

change is attributable to photochemical ligand substitution of the Ru(II) photosensitizer unit giving the corresponding Ru(II) bisdiimine-type complex(es).[29,30] This should be a main reason why the rate of photocatalytic formic acid production using **RuReCl** gradually decreased. For clarifying details of the photochemical decomposition process of the Ru(II) complexes in the presence of sodium ascorbate, photolysis experiments of **Ru** were conducted in an aqueous solution containing sodium ascorbate (200 mM) or $NaHCO_3$ (5 mM) under a CO_2 atmosphere (the pH of both solutions was 5.5). In the presence of sodium ascorbate, faster decomposition of **Ru** was observed than that in the presence of $NaHCO_3$ (see Figures 9a and 9b). The absorption spectrum of the ligand-substitution product in the case of the $NaHCO_3$ solution was similar to that of $[Ru(bpy)_2(OH_2)_2]^{2+}$ (orange line in Figures 9c and 9d). However, the addition of sodium ascorbate induced a drastic change of the UV-vis absorption spectrum of $[Ru(bpy)_2(OH_2)_2]^{2+}$, as shown by the blue line in Figure 9d. This absorption spectrum of the produced Ru(II) complex with ascorbate as a ligand or ligands was similar to that obtained by the photoirradiated solution of **Ru** in the presence of sodium ascorbate (see the blue line in Figure 9c). These results indicate that one of the deactivation processes of the **RuReCl** photocatalyst in the aqueous solution is the photochemical conversion of the photosensitizer unit to the Ru(II) bisdiimine complex(es) with an ascorbate ligand or ligands.

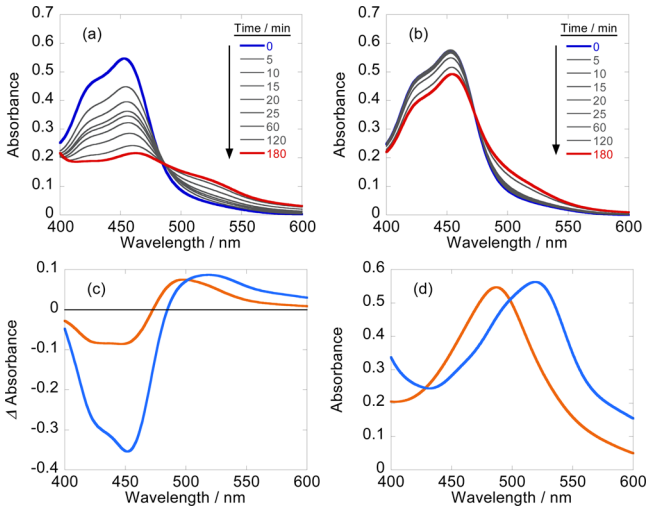

Figure 9. UV-vis absorption spectral changes of aqueous solutions (pH 5.5) containing **Ru** (0.05 mM) in the presence of (a) sodium ascorbate (200 mM) or (b) $NaHCO_3$ (5 mM) during irradiation. (c) Differential absorption spectra between before and after the irradiation for 180 min in the cases of panel (a) (blue) and panel (b) (orange). (d) Absorption spectra of aqueous solutions containing of $Ru(bpy)_2(OH_2)_2^{2+}$ (0.05 mM) before (orange) and after (blue) the addition of sodium ascorbate (200 mM).

CONCLUSION

RuReCl acted, as a photocatalyst for CO_2 reduction even in an aqueous solution. However, the product was totally different from that in an organic solution: formic acid in the aqueous solution with ascorbate as a reductant, rather than CO in a DMF–TEOA mixed solution with BNAH as a reductant. One of the main reasons for the relatively low efficiency of the photocatalytic reaction in the aqueous solution was the rapid BET from the OERS of the photosensitizer unit to the oxidized ascorbate both before and after the production of the OERS, which escaped from the solvent cage. The photocatalyst was gradually decomposed to give the corresponding Ru(II) bisdiimine complex(es) in the aqueous solution. Therefore, the photocatalysis (efficiency and selectivity) using supramolecules in an aqueous media should be improved by suppression of both the BET and the decomposition process of the photosensitizer unit. From these view points, further studies are now underway.

EXPERIMENTAL SECTION

General Procedures. Infrared (IR) spectra were measured with a JASCO Model FT/IR-610 spectrophotometer using a resolution of 1 cm^{-1}. UV-vis absorption spectra were measured with a JASCO Model V-565 spectrophotometer. Emission spectra were measured at 298 ± 0.1 K with a JASCO Model FP-6500 spectrofluorometer. The emission quantum yields were measured with a Hamamatsu photonics C-9920-02 using a multiphotodiode-array detector. Emission lifetimes were measured with a Horiba FluoroCube 1000U-S time-correlated single-photon-counting system (the excitation source was a nano-LED 460, and the instrument response was <1 ns).

Proton NMR spectra were measured in an acetone-d_6 or CD_3OD solution using a JEOL Model AL300 (300 MHz) system. Proton NMR spectra using a standard-solvent method (No-D) were measured in a H_2O solution, using a JEOL Model ECX400 (400 MHz) system. Carbon NMR spectra were measured in a H_2O solution, using a JEOL Model ECX400 (100 MHz) system. Electrospray ionization–mass spectroscopy (ESI-MS) was performed with a Shimadzu Model LCMS-2010A system, using HPLC-grade MeCN or MeOH as a mobile phase.

Cyclic voltammograms were measured in an MeCN solution containing NEt_4BF_4 (0.1 M) as a supporting electrolyte, using an ALS/CHI Model CHI-720 electrochemical analyzer with a grassy-carbon disk working electrode (3 mm diameter), a Pt counter electrode, and a $Ag/AgNO_3$ (0.01 M) reference electrode.

Time-resolved UV-vis absorption spectroscopy was employed to measure the transient absorption spectra and corresponding time constants. The excitation light source was a Spectra-Physics LAB-150-10 Nd^{3+}:YAG pulse laser with the attenuator consists of the Glan-Laser prism and the $\lambda/2$ wave plate (second-harmonic generation at 532 nm, 10 ns fwhm, 5–20 mJ $pulse^{-1}$). The monitoring light beam was passed through the quartz cuvette (10 mm × 10 mm × 40 mm) and led into a Model R926 photomultiplier tube (Hamamatsu Photonics) on a Jobin–Yvon Model HR-320 monochromator. Time profiles of the monitoring light intensity were stored using a LeCroy WaveRunner 640zi oscilloscope (4-GHz bandwidth). A Ushio Model 300-WXe arc lamp was operated in a pulse-enhanced mode (500-μs duration), with an XC-300 power supply and an YXP-300 light pulsar (Eagle Shoji, Inc.) as the monitoring light source. The sample solutions for laser photolysis were degassed by the freeze–pump–thaw method.

Materials. Acetonitrile was distilled over P_2O_5 three times and then distilled over CaH_2. DMF was dried over molecular sieve 4A, and distilled under reduced pressure (10–20 Torr). TEOA was distilled under reduced pressure (<1 Torr) under argon before use. Water was purified using Millipore Elix Essential 3 UV System from tap water. All of the purified solvents except water were kept under an argon atmosphere. Other materials were reagent-grade quality and were used without further purification.

Synthesis. 1-Benzyl-1,4-dihydronicotinamide (BNAH), 1,2-bis(4′-methyl-[2,2′-bipyridin]-4-yl)ethane (**C2**),[31] 4,4′-bis-(diethylmethylphosphonate)-2,2′-bipyridine (**bpy($CH_2PO_3Et_2$)$_2$**),[32] $[Ru(bpy)_3]Cl_2$ (**Ru**),[33] and $[Ru(bpy)_2(OH_2)_2](OTf)_2$[34] were prepared according to the literature.

[Rubpy$_2$(MebpyCH$_2$CH$_2$bpyMe)Re(CO)$_3$Cl]Cl$_2$·8H$_2$O (**RuReCl**). $[Ru(bpy)_2(MebpyCH_2CH_2bpyMe)Re(CO)_3Cl](PF_6)_2$ was synthesized according to the method described in the literature.[11] The PF_6^- salt

DOI: 10.1021/ic502707t
Inorg. Chem. 2015, 54, 1800–1807

was treated with the Cl^- form of an Amberlite IRA-900J ion-exchange resin to give the corresponding Cl^- salts, which were recrystallized with MeOH-Et_2O. Anal. Calcd for $C_{47}H_{54}Cl_3N_8O_{11}ReRu$: C, 43.40; H, 4.18; N, 8.62. Found: C, 43.70; H, 4.26; N, 8.90. FT-IR (MeCN) ν_{CO} (cm^{-1}): 2021, 1915, 1896. ESI-MS (Eluent: MeOH) m/z: 543 ($[M-2Cl^-]^{2+}$).

*[Re{bpy(CH$_2$PO$_3$H$_2$)$_2$}(CO)$_3$Cl]·4H$_2$O (**ReCl**).* A toluene solution (10 mL) containing $Re(CO)_5Cl$ (93.2 mg, 0.26 mmol) and bpy-$(CH_2PO_3Et_2)_2$ (130 mg, 0.28 mmol) was refluxed at 110 °C for 2 h. After cooling to room temperature, the reaction solution was filtered to afford yellow solid. An HCl aqueous solution (18%, 50 mL) was added to it and refluxed at 100 °C for 18 h. After removal of the solvent by evaporation, the precipitate was washed with 10 mL of acetone. Anal. Calcd for $C_{15}H_{32}ClN_2O_{13}P_2Re$: C, 24.95; H, 3.07; N, 3.88. Found: C, 24.60; H, 2.83; N, 4.04. ^1H NMR (297.60 MHz, DMSO) δ/ppm: 8.90 (d, 2H, J = 5.8 Hz), 8.53 (s, 2H), 7.63 (d, 2H, J = 5.8 Hz), 3.30 (d, 2H, $^2J_{P-H}$ = 22.4 Hz). FT-IR (DMF) ν_{CO} (cm^{-1}): 2018, 1914, 1890.

Photocatalytic Reactions. The Cl^- salt of **RuReCl** was used because of the low solubility of the corresponding PF_6^- salts in water. Photocatalytic reactions were performed in an 11-mL test tube (inner diameter (ID) of 8 mm) containing 4 mL of an aqueous solution of the metal complexes (0.05 mM) and sodium ascorbate (200 mM) after purging with CO_2 for 30 min. The solutions were irradiated using a merry-go-round irradiation apparatus at λ > 500 nm with a high-pressure Hg lamp combined with a K_2CrO_4 (30 wt %, diameter (d) of 1 cm) solution filter. Formation quantum yields of formic acid were determined by the following method. The reaction solution in a quartz cubic cell (light pass: 1 cm) was irradiated under a CO_2 atmosphere using a Ushio Optical Modulex high-pressure Hg lamp (Model BA-H500) combined with a 546 nm (fwhm = 10 nm) band-pass filter purchased from Asahi Spectra Co. and a 5-cm-long $CuSO_4$ solution (250 g L^{-1}) filter. The temperatures of the solutions were controlled at 298 ± 2 K using an IWAKI constant temperature system (Model CTS-134A) during irradiation. The gaseous reaction products, i.e., CO and H_2, were analyzed by gas chromatography−thermal conductivity detection (GC-TCD) (GL Science, Model GC 323). HCOOH in the liquid phase was analyzed by a capillary electrophoresis system (Otsuka Electronics Co., Model Capi-3300I).

$^{13}CO_2$-Labeling Experiment. The $^{13}CO_2$ labeling experiments were performed using 1 mL of an aqueous solution containing **RuReCl** (0.5 mM) and sodium ascorbate (200 mM) in a test tube (ID = 1 cm). The tube was degassed using the freeze−pump−thaw method, and then $^{13}CO_2$ (707 Torr) was introduced to it. No-D ^1H NMR and ^{13}C NMR spectra were measured before and after 18-h irradiation.

■ ASSOCIATED CONTENT

Ⓢ Supporting Information

Kinetic analysis methods, Stern−Volmer plots, quantum yield measurements, and time causes of the products. This material is available free of charge via the Internet at http://pubs.acs.org.

■ AUTHOR INFORMATION

Corresponding Author

*E-mail: ishitani@chem.titech.ac.jp.

Present Address

$^{\nabla}$1404-1 Katakura, Hachioji, Tokyo 192−0982, Japan.

Notes

The authors declare no competing financial interest.

■ ACKNOWLEDGMENTS

This work was partially supported by a Grant-in-Aid for Scientific Research on Innovative Areas, "Artificial Photosynthesis (AnApple)" (No. 24107005), from the Japan Society for the Promotion of Science (JSPS).

■ REFERENCES

(1) Grant, J. L.; Goswami, K.; Spreer, L. O.; Otvos, J. W.; Calvin, M. *J. Chem. Soc., Dalton Trans.* **1987**, *9*, 2105−2109.
(2) Craig, C. A.; Spreer, L. O.; Otvos, J. W.; Calvin, M. *J. Phys. Chem.* **1990**, *94*, 7957−7960.
(3) Kimura, E.; Bu, X.; Shionoya, M.; Wada, S.; Maruyama, S. *Inorg. Chem.* **1992**, *31*, 4542−4546.
(4) Kimura, E.; Wada, S.; Shionoya, M.; Okazaki, Y. *Inorg. Chem.* **1994**, *33*, 770−778.
(5) Mochizuki, K.; Manaka, S.; Takeda, I.; Kondo, T. *Inorg. Chem.* **1996**, *35*, 5132−5136.
(6) Tinnemans, A. H. A.; Koster, T. P. M.; Thewissen, D. H. M. W.; Mackor, A. *Recl. Trav. Chim. Pays-Bas* **1984**, *103*, 288−295.
(7) Boston, D. J.; Xu, C.; Armstrong, D. W.; MacDonnell, F. M. *J. Am. Chem. Soc.* **2013**, *135*, 16252−16255.
(8) Ikuta, N.; Takizawa, S.; Murata, S. *Photochem. Photobiol. Sci.* **2014**, *13*, 691−702.
(9) Gholamkhass, B.; Mametsuka, H.; Koike, K.; Tanabe, T.; Furue, M.; Ishitani, O. *Inorg. Chem.* **2005**, *44*, 2326−2336.
(10) Sato, S.; Koike, K.; Inoue, H.; Ishitani, O. *Photochem. Photobiol. Sci.* **2007**, *6*, 454−461.
(11) Koike, K.; Naito, S.; Sato, S.; Tamaki, Y.; Ishitani, O. *J. Photochem. Photobiol. A: Chem.* **2009**, *207*, 109−114.
(12) Tamaki, Y.; Watanabe, K.; Koike, K.; Inoue, H.; Morimoto, T.; Ishitani, O. *Faraday Discuss.* **2012**, *155*, 115−127.
(13) Takeda, H.; Ishitani, O. *Coord. Chem. Rev.* **2010**, *254*, 346−354.
(14) Tamaki, Y.; Morimoto, T.; Koike, K.; Ishitani, O. *Proc. Natl. Acad. Sci. U.S.A.* **2012**, *109*, 15673−15678.
(15) Sekizawa, K.; Maeda, K.; Domen, K.; Koike, K.; Ishitani, O. *J. Am. Chem. Soc.* **2013**, *135*, 4596−4599.
(16) Tamaki, Y.; Koike, K.; Morimoto, T.; Ishitani, O. *J. Catal.* **2013**, *304*, 22−28.
(17) Creutz, C.; Sutin, N.; Brunschwig, S. B. *J. Am. Chem. Soc.* **1979**, *101*, 1297−1298.
(18) Brown, M. G.; Brunschwig, S. B.; Creutz, C.; Endicott, F. J.; Sutin, N. *J. Am. Chem. Soc.* **1979**, *101*, 1298−1300.
(19) Shan, B.; Baine, T.; Ma, N. X.; Zhao, X.; Schmehl, H. R. *Inorg. Chem.* **2013**, *52*, 4853−4859.
(20) Two conflict results have been reported on quenching of the excited **Ru** by ascorbic acid (not ascorbate); some papers[7,35,36] have described strong dependence of the quenching rate on pH of the solution, but one[19] reported no such dependence. We carefully checked this and concluded that **Ru** is efficiently quenched by ascorbate but less efficiently quenched by ascorbic acid (see Figure S1 in the Supporting Information).
(21) Miedlar, K.; Das, P. K. *J. Am. Chem. Soc.* **1982**, *104*, 7462−7469.
(22) Krishnan, C. V.; Sutin, N. *J. Am. Chem. Soc.* **1981**, *103*, 2141−2142.
(23) Haynes, W. N. *CRC Handbook of Chemistry and Physics*, 95th Edition; CRC Press: Boca Raton, FL, 2014
(24) Bielski, J. B.; Allen, O. A.; Schwarz, A. H. *J. Am. Chem. Soc.* **1981**, *103*, 3516−3518.
(25) Guttentag, M.; Rodenberg, A.; Kopelent, R.; Buchwalder, C.; Brandstätter, M.; Hamm, P.; Alberto, R. *Eur. J. Inorg. Chem.* **2012**, 59−64.
(26) Guttentag, M.; Rodenberg, A.; Bachmann, C.; Senn, A.; Hamm, P.; Alberto, R. *Dalton. Trans.* **2013**, *42*, 334−337.
(27) Bachmann, C.; Probst, B.; Guttentag, M.; Alberto, R. *Chem. Commun.* **2014**, *50*, 6737−6739.
(28) Konno, H.; Kobayashi, A.; Sakamoto, K.; Fagalde, F.; Katz, N. E.; Saitoh, H.; Ishitani, O. *Inorg. Chim. Acta* **2000**, *299*, 155−163.
(29) Van Houten, J.; Watts, R. J. *Inorg. Chem.* **1978**, *17*, 3381−3385.
(30) Porter, G. B.; Hoggard, P. E. *J. Am. Chem. Soc.* **1978**, *100*, 1457−1463.
(31) Ferrere, S.; Elliott, C. M. *Inorg. Chem.* **1995**, *34*, 5818−5824.
(32) Jurss, J. W.; Concepcion, J. C.; Norris, M. R.; Templetion, J. L.; Meyer, T. J. *Inorg. Chem.* **2010**, *49*, 3980−3982.
(33) Mabrouk, P. A.; Wrighton, M. S. *Inorg. Chem.* **1986**, *25*, 526−531.

DOI: 10.1021/ic502707t
Inorg. Chem. 2015, 54, 1800−1807

(34) Taher, D.; Thibault, M. E.; Di mondo, D.; Jennings, M.; Schlaf, M. *Chem. Eur.—J.* **2009**, *15*, 10132−10143.
(35) Fukuzumi, S.; Kobayashi, T.; Suenobu, T. *Angew. Chem., Int. Ed.* **2011**, *50*, 728−731.
(36) Sano, Y.; Onoda, A.; Hayashi, T. *Chem. Commun.* **2011**, *47*, 8229−8231.

DOI: 10.1021/ic502707t
Inorg. Chem. 2015, 54, 1800−1807